Dynamics of proteins by NMR

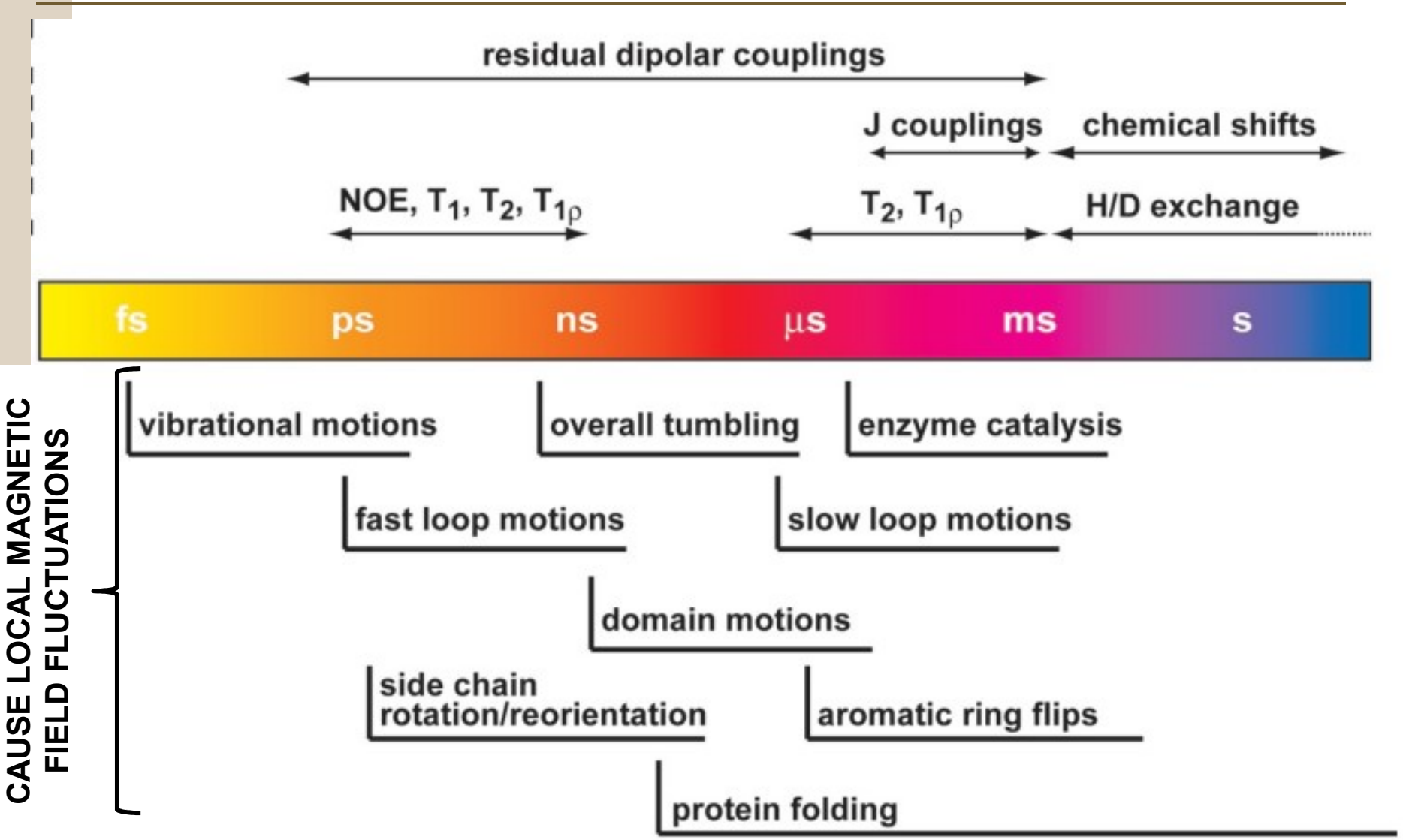

Correlation Functions of Small and Large Molecules

-slow fluctuations
-large molecules
-low temperature
-high viscosity
-longer τ_c

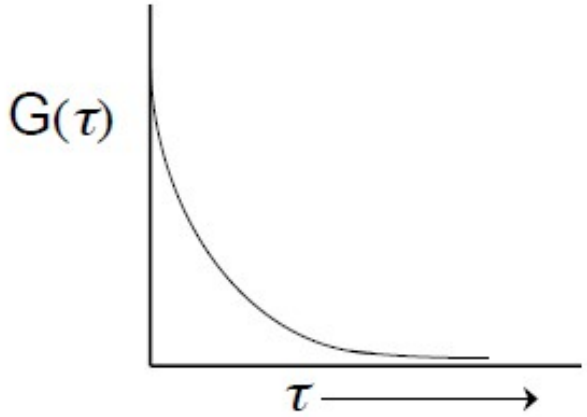

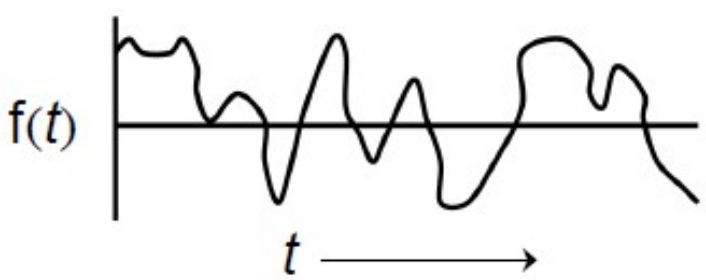

-fast fluctuations
-small molecules
-high temperature
-low viscosity
-shorter τ_c

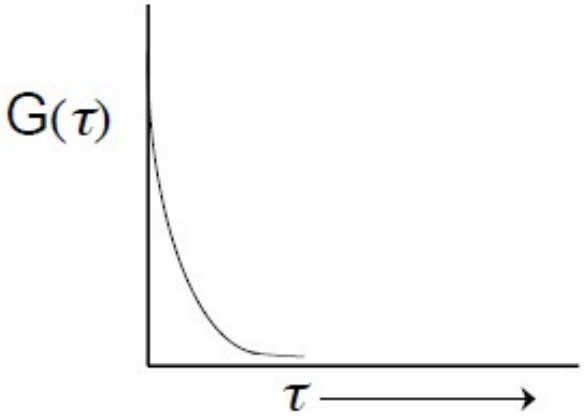

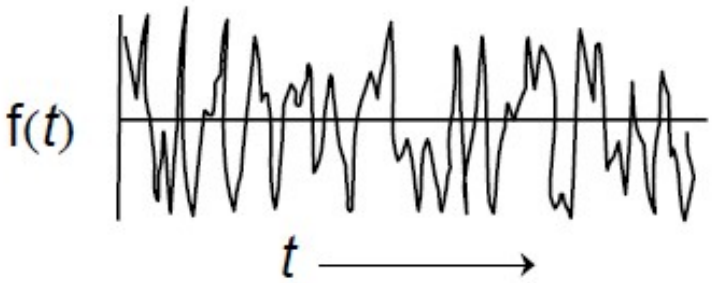

Protein Dynamics by NMR: relaxation rates

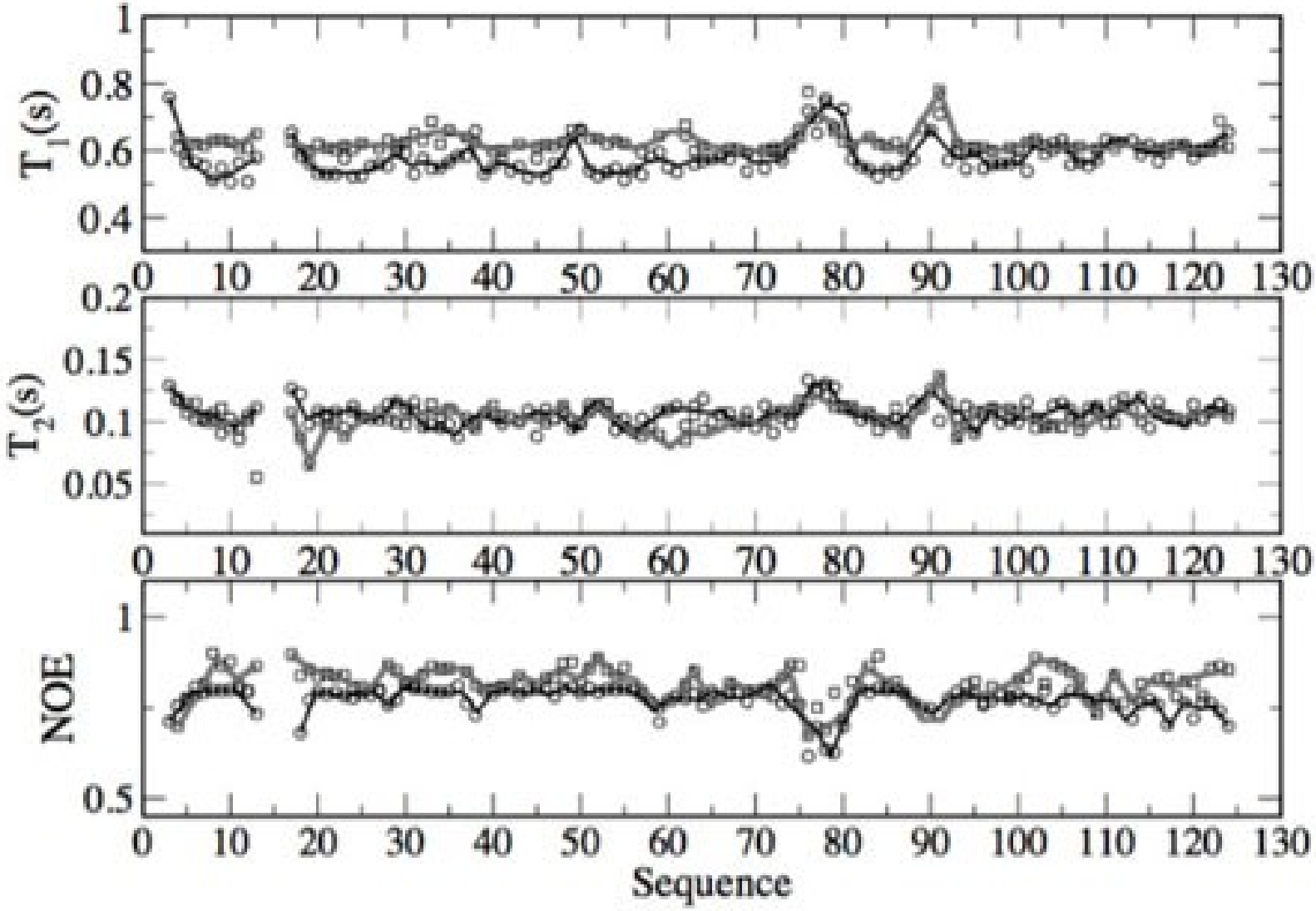

Protein Dynamics by NMR: relaxation rates

Catabolite activator protein (CAP^N)

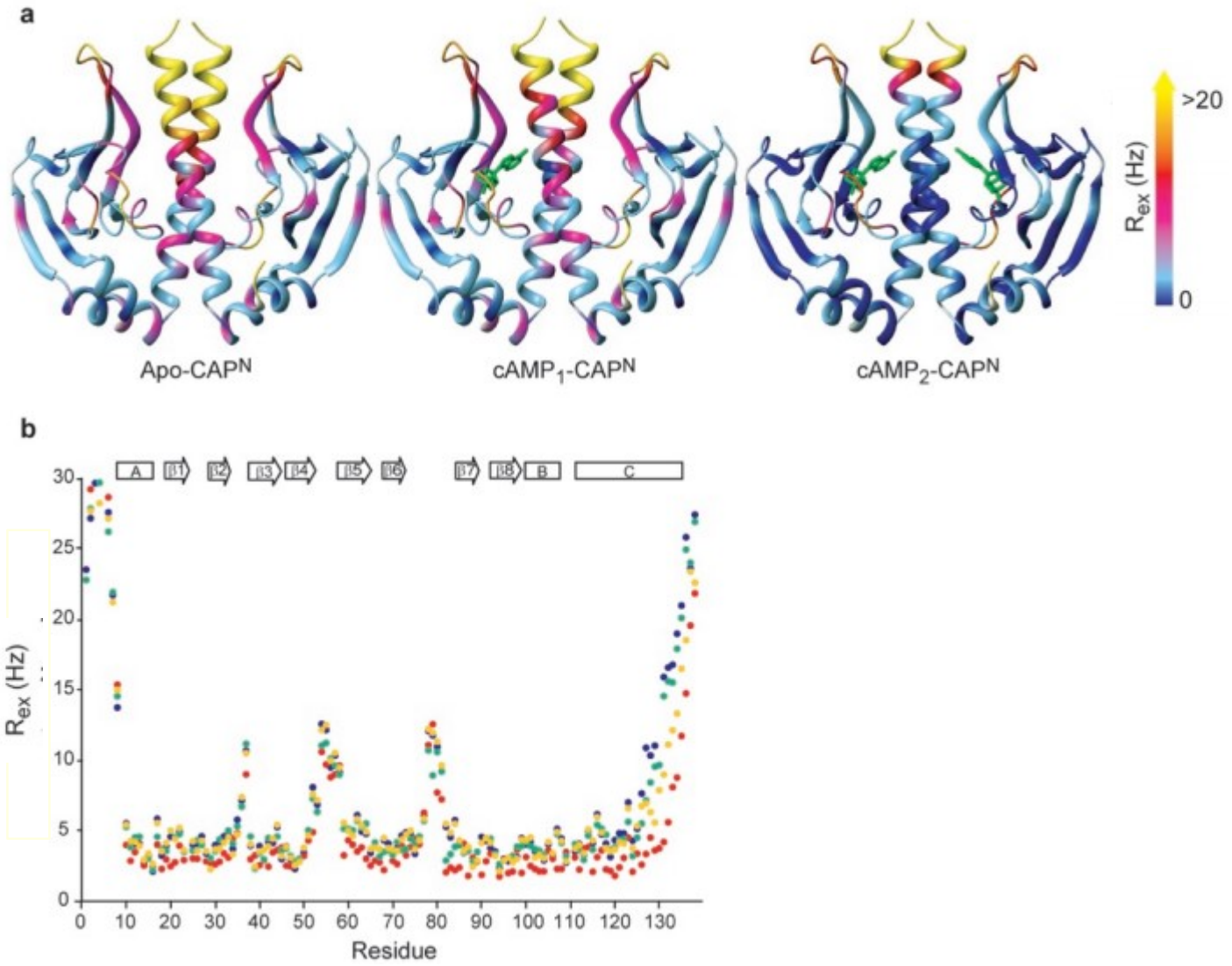

Molecular dynamics (spin-relaxation)

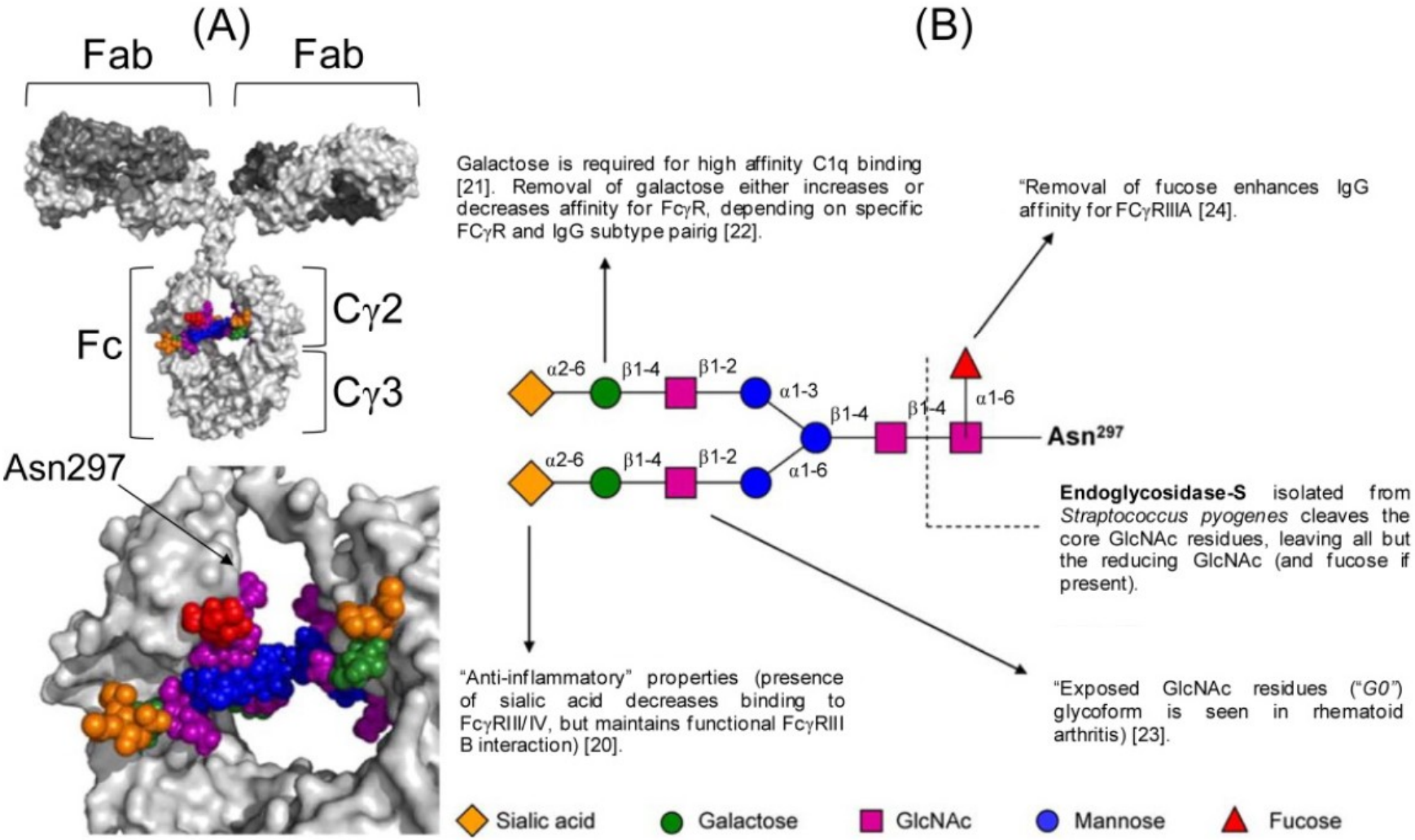

Molecular dynamics (spin-relaxation)

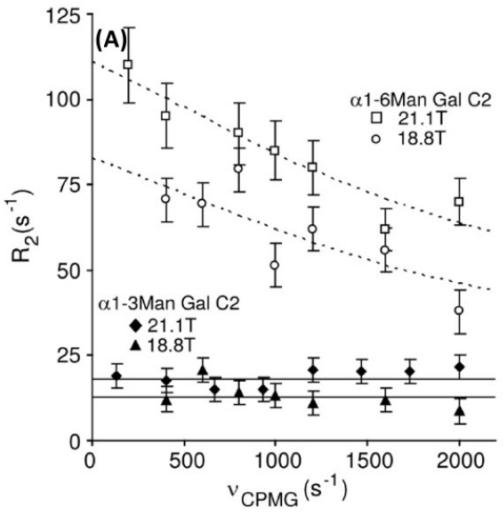

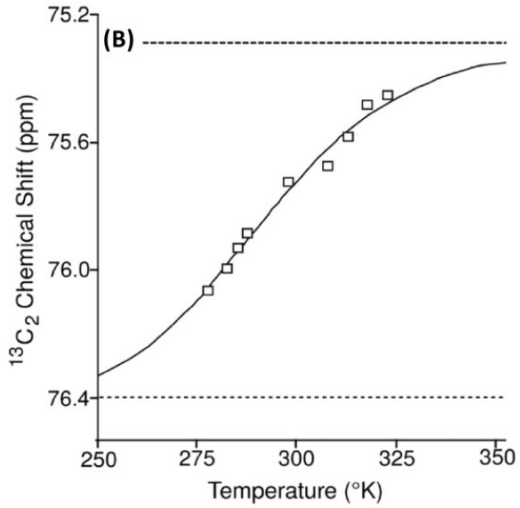

	α1-3Man-linked	α1-6Man-linked
	Relaxation rates	Relaxation rates
900 MHz	**Galactose ^{13}C6**	**Galactose ^{13}C6**
R_1	2.8 ±0.1 s^{-1}	3.1 ±0.4 s^{-1}
R_2	48.4 ±5.5 s^{-1}	59.7 ±9.2 s^{-1}
900 MHz	**Galactose ^{13}C2**	**Galactose ^{13}C2**
R_1	1.2 ±0.1 s^{-1}	1.2 ±0.2 s^{-1}
$R_{1\rho}$	20.1 ±1.0 s^{-1}	56.1 ±10 s^{-1}
$R_{2\ linewidths}$	40 s^{-1}	150 s^{-1}
600 MHz		
$R_{1\rho}$	14.7 ±1.1 s^{-1}	48.0 ±5.4 s^{-1}
$R_{2\ linewidths}$	28 s^{-1}	107 s^{-1}
R_2	29 s^{-1}	ND

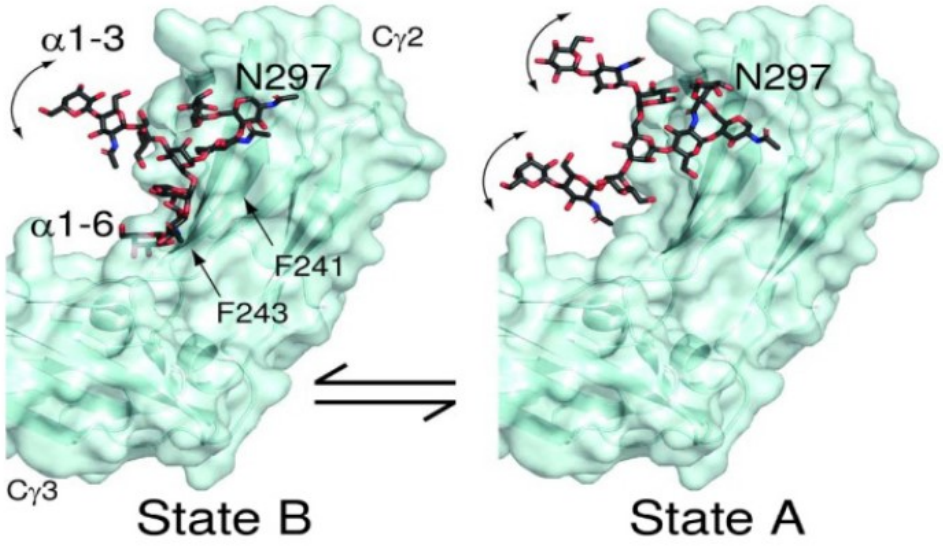

Ring and chain conformations and dynamics of native SF, SG and derived oligosaccharides

Dynamics determined by ^{1}H1 spin-relaxation

Table III.

Longitudinal spin relaxation (T_1) (in s) of the anomeric ^{1}H signals of *Lv* I, *Lv* II and *Lv* III signals from the oligosaccharide mixture from Structure 2

	^{1}H T_1 (s)[a]		
	298 K	**310 K**	**323 K**
Anomeric unit (sulfation type)	*Lv* I (octasaccharide, Structure 1)		
A H1 (2-sulfated)	1.13	1.15	1.31
B H1 (2,4-disulfated)	1.06	1.07	1.30
C H1 (2-sulfated)	1.17	1.23	1.31
D H1 (4-sulfated)	1.26	1.30	1.36
A′ H1 (unsulfated)	1.30	1.36	1.37

GLYCOBIOLOGY

Ismael NL Queiroz et al. Glycobiology 2015;25:535-547

Ring and chain conformations and dynamics of native SF, SG and derived oligosaccharides

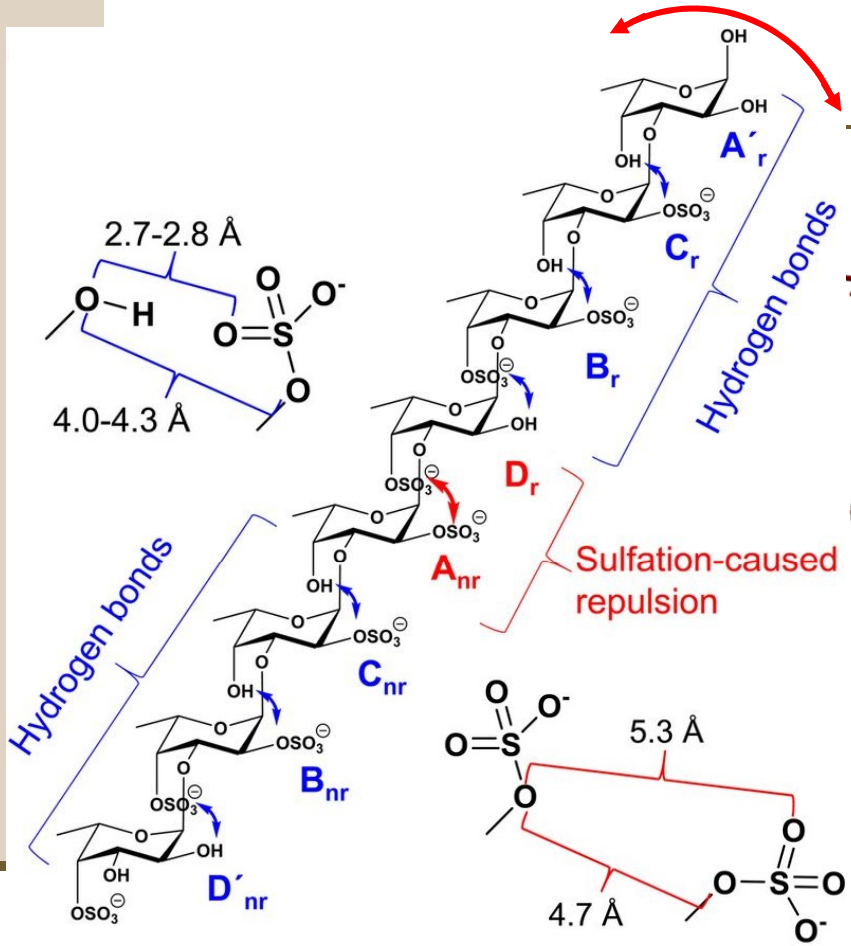

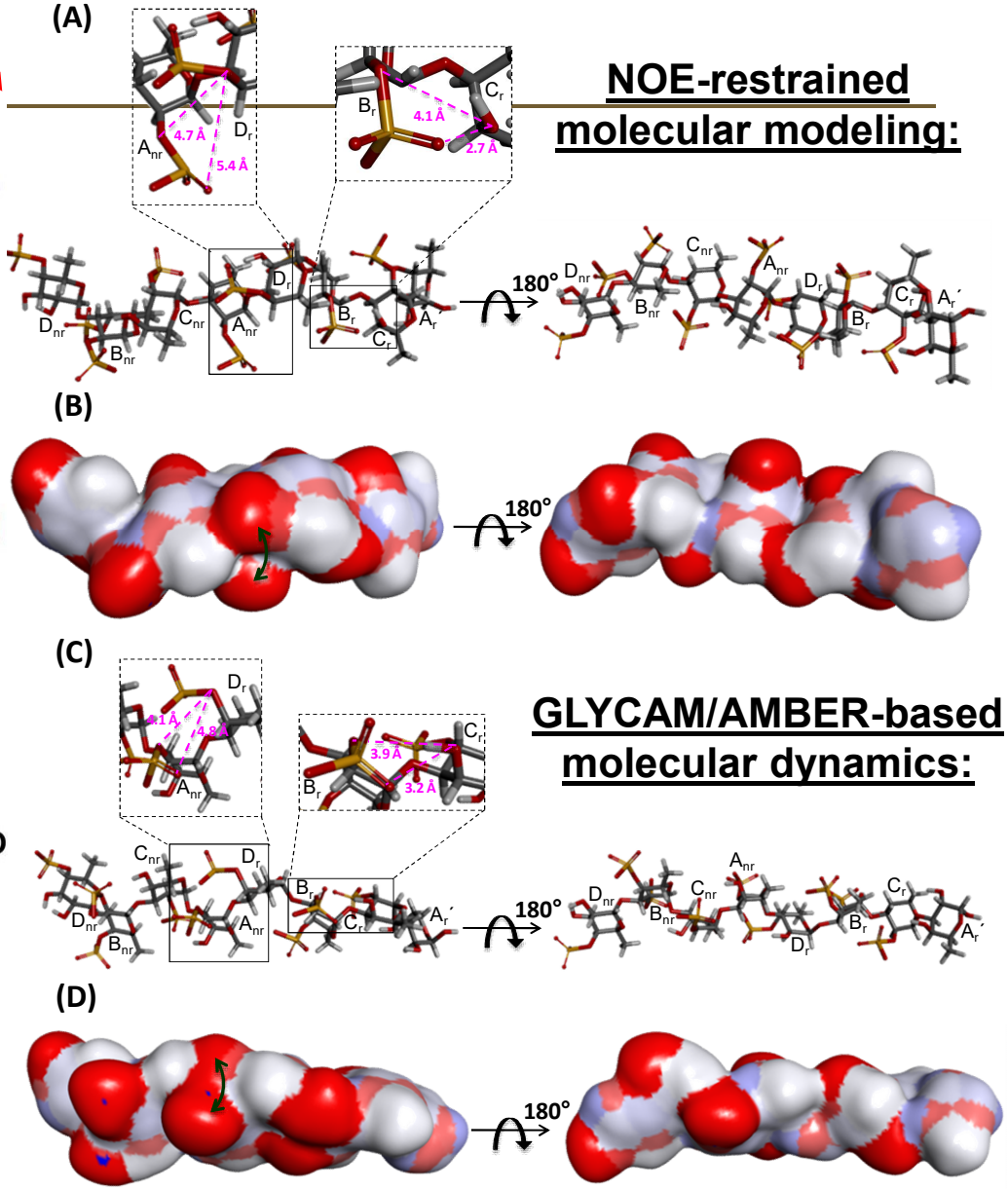

GLYCOBIOLOGY

Ismael NL Queiroz et al. Glycobiology 2015;25:535-547

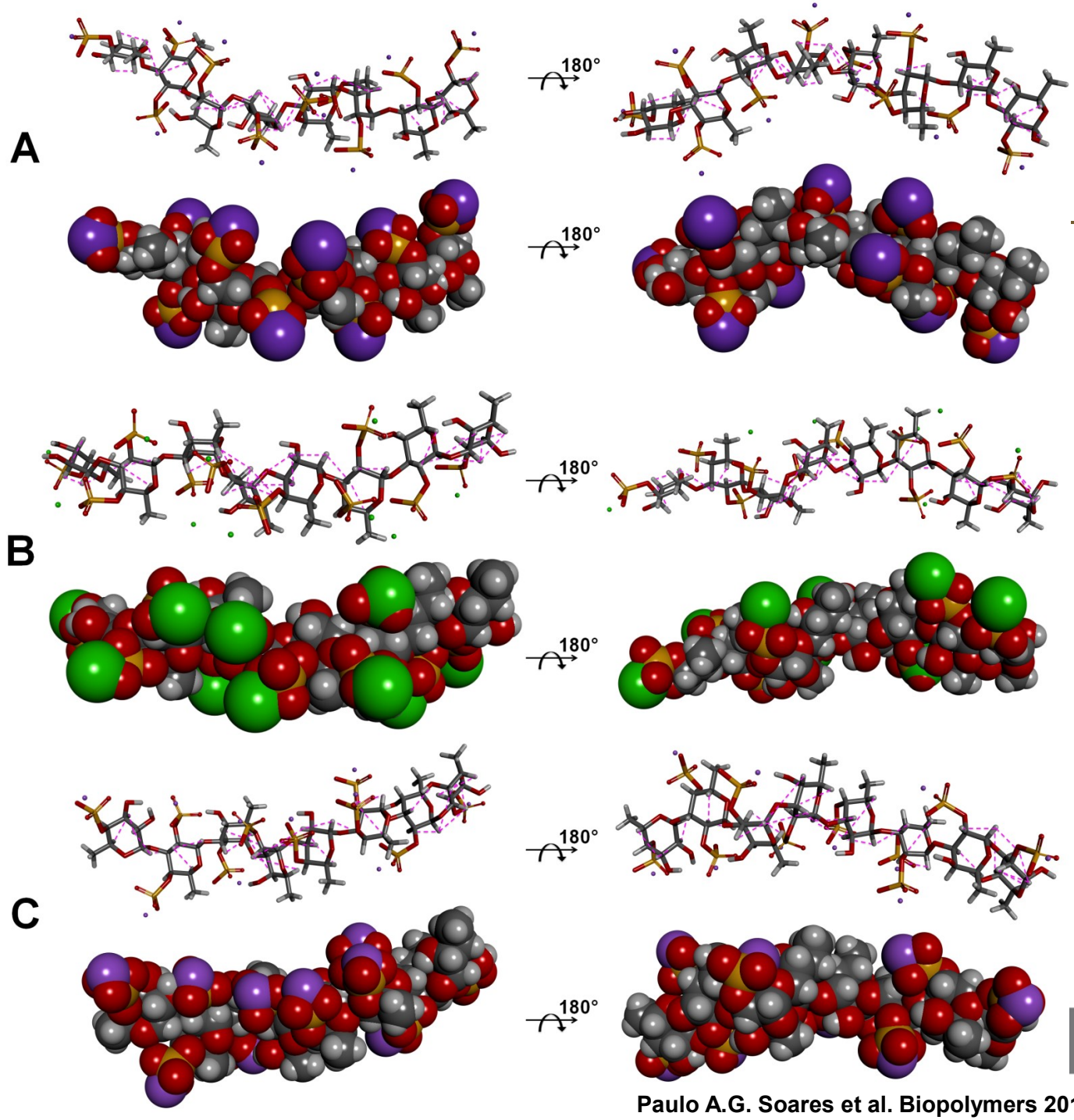

Biopolymers

Paulo A.G. Soares et al. Biopolymers 2016;105:840-851

Ring and chain conformations and dynamics of native SF, SG and derived oligosaccharides

Counterion effects (Na^+, Ca^{2+}, Li^+)

Table VI Spin-spin relaxation rate (R_2) and rotational spin-lattice relaxation rate ($R_{1\rho}$) (in sec^{-1}) of the anomeric ^1H signals from the differently sulfated Fuc*p* units in the Na^+-, Ca^{2+}- and Li^+-substituted sulfated fucan preparations at two different temperatures (298 and 310 K) at a Bruker 600 MHz.

Signals	^1H R_2 (s^{-1})[a]	
	298K	310K
Na^+-sulfated fucan		
A_{H1}/B_{H1}	257.7 ±3	227.3 ±5
C_{H1}	283.8 ±5	244.4 ±6
D_{H1}	272.5 ±5	237.0 ±5
Ca^{2+}-sulfated fucan		
A_{H1}/B_{H1}	166.6 ±9	160.2 ±3
C_{H1}	189.5 ±6	177.4 ±14
D_{H1}	182.3 ±6	178.3 ±13
Li^+-sulfated fucan		
A_{H1}/B_{H1}	208.7 ±3	179.2 ±4
C_{H1}	240.5 ±12	204.0 ±10
D_{H1}	213.1 ±7	186.5 ±4

Signals	^1H $R_{1\rho}$ (s^{-1})[b]	
	298K	310K
Na^+-sulfated fucan		
A_{H1}/B_{H1}	102.6 ±3	98.7 ±4
C_{H1}	109.7 ±4	99.6 ±1
D_{H1}	106.5 ±2	88.7 ±2
Ca^{2+}-sulfated fucan		
A_{H1}/B_{H1}	88.8 ±4	87.9 ±1
C_{H1}	91.0 ±4	90.9 ±3
D_{H1}	92.9 ±2	88.7 ±2
Li^+-sulfated fucan		
A_{H1}/B_{H1}	96.9 ±3	84.1 ±2
C_{H1}	101.2 ±2	88.1 ±3
D_{H1}	99.4 ±4	87.1 ±6

Biopolymers

Paulo A.G. Soares et al. Biopolymers 2016;105:840-851

Ring and chain conformations and dynamics of native SF, SG and derived oligosaccharides

Conformation and dynamics of oligosaccharides from the 3-linked 2-sulfated alpha-L-SF (*S. franciscanus*) and alpha-L-SG (*E. lucunter*) with similar MWs

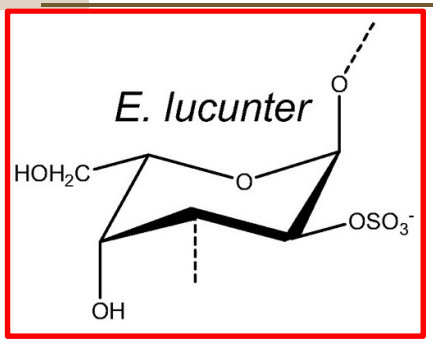

vs

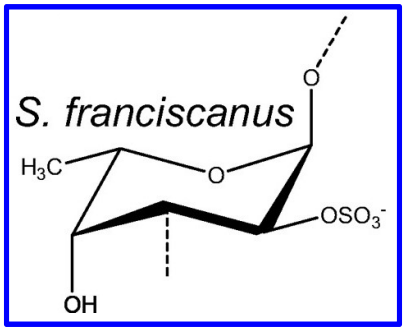

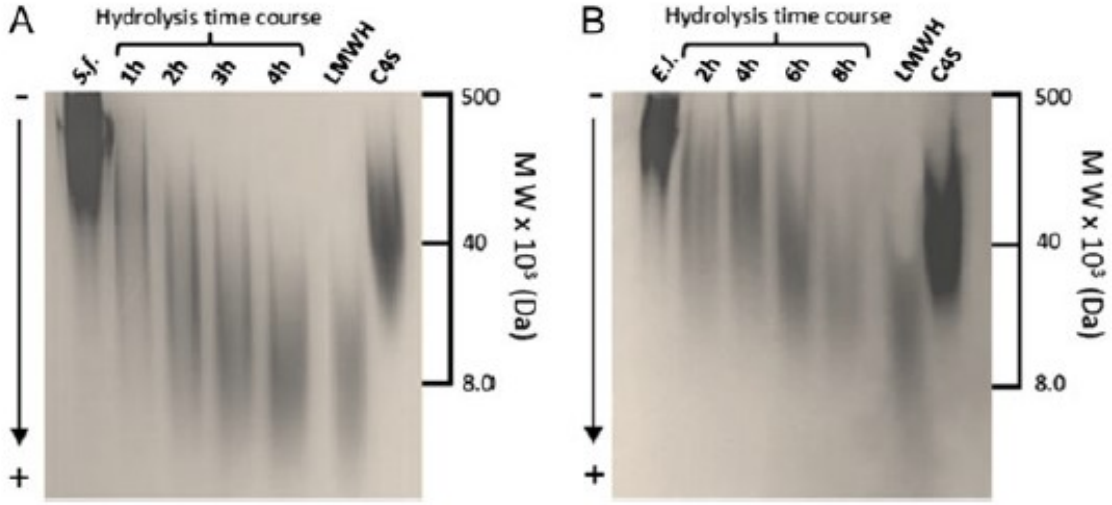

Table III. Spin-lattice (R_1) and spin–spin (R_2) relaxation rates (both measured in s^{-1}) measured at 298 K for the fractionated oligosaccharides *S.f.* XII and *S.f.* VIII, and the mixtures of unfractionated oligosaccharides, *S.f.* Hd and *E.l.* Hd, produced respectively from the hydrolyzed SF and SG samples

Type	Resonance	R_1[a]	R_2[b]	Resonance	R_2
S.f. Hd	A1	0.8	32.2	B1	36.0
	A2	0.5	35.5	B2	36.6
	A3/A4	0.5	36.6	B3/B4	39.8
	A5	0.7	35.1	B5	41.0
	A6	0.7	33.6	B6	32.2
S.f. XII	A1	0.4	26.3	B1	35.4
	A2	0.5	27.5	B2	33.5
	A3/A4	0.3	20.9	B3/B4	34.0
	A5	1.0	25.4	B5	35.4
	A6	0.3	22.0	B6	36.8
S.f. VIII	A1	0.8	30.0	B1	38.9
	A2	Nd[c]	37.2	B2	35.5
	A3/A4	0.6	29.4	B3/B4	35.3
	A5	Nd	32.9	B5	32.9
	A6	0.6	35.0	B6	46.9
E.l. Hd	A1	1.2	41.3	B1	42.4
	A2	1.4	34.4	B2	44.4
	A3	1.6	Nd	B3	52.0
	A4	1.6	32.6	B4	41.8
	A5	1.5	37.6	B5	Nd
	A6	1.0	39.9	B6	48.6

[a]Longitudinal relaxation rates (R_1) were measured from $1/T_1$ of each resonance after applying NMR 1D ^{1}H inversion recovery experiment as described in Materials and methods.

[b]Transverse relaxation rates (R_2) were measured as ^{1}H1-linewidths ($\upsilon_{1/2}$, width at half height) of each resonance using the following equations: $\upsilon_{1/2} = 1/\pi T_2 \rightarrow R_2 = 1/T_2$, ($\upsilon_{1/2}$ in Hz, T_2 in s, and R_2 in s^{-1}).

[c]Not determined.

GLYCOBIOLOGY

Ismael NL Queiroz et al. Glycobiology 2016; *6:1257-1264*

FUCANOMICS & GALACTANOMICS: STRUCTURE *vs* FUNCTION

Structure-anticoagulant activity relationship: SUGAR TYPE-DEPENDENT ACTION

(i) *E. lucunter*

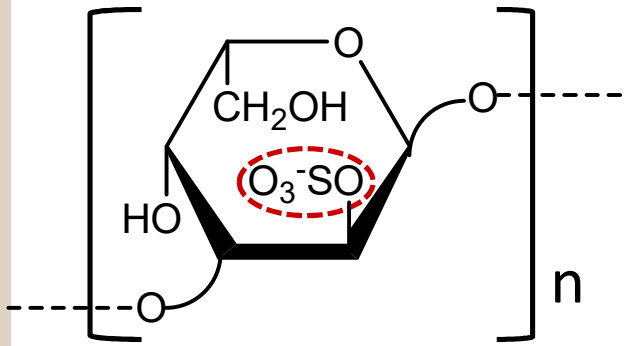

VS

(h) *S. franciscanus*

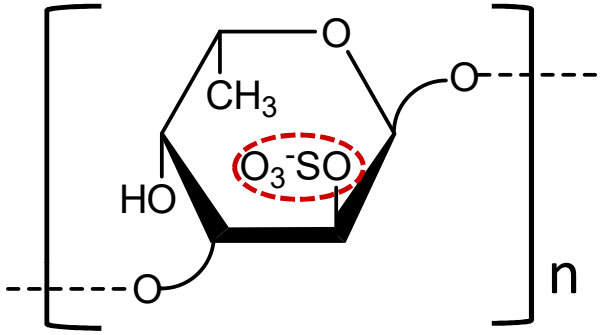

Vitor H. Pomin – **Marine Regular Sulfated Homopolysaccharides.** Biopolymers **2009**, Volume 91, Issue 8:601-609.

FUCANOMICS & GALACTANOMICS: STRUCTURE *vs* FUNCTION

Table I. Anticoagulant Activities of Marine Invertebrate and Algal Sulfated Fucans and Sulfated Galactans Measured by APTT[a] and by IC_{50} for Thrombin (IIa) and Factor Xa Inhibition in the Presence of Antithrombin (AT) or Heparin Cofactor II (HCII)21, 48

				IC_{50} (μg ml^{-1})		
Polysaccharide	Source	Structure (Figure)	APTT (IU mg^{-1})	IIa/AT	IIa/HCII	Xa/AT
3-Linked sulfated α-L-fucans	*S. purpuratus* (I)	1E-I	76	0.3	0.3	2
	S. purpuratus (II)	1E-II	10	0.9	2	ND
	S. pallidus	1C	18	>500	>500	>500
	L. variegatus	1B	3	>500	>500	>500
	S. franciscanus	1G	~2	>500	>500	250
	L. grisea	1A	<1	>500	>500	>500
4-Linked sulfated α-L-fucans	*S. droebachiensis*	1F	<1	ND	ND	ND
	A. lixula	1D	~2	150	150	>500
Sulfated α-L-galactans	*E. lucunter*	2A	20	3	6	20
	H. monus	2C	~2	>500	>500	>500
	S. plicata	2B	<1	>500	>500	>500
Algal sulfated galactans15, 19	*B. occidentalis*	2D	93	0.02	1.1	2.5
	G. crinale		65	0.02	25	1.5

a The activity is expressed as international U mg^{-1} using a parallel standard curve based on the International Heparin Standard (193 U mg^{-1}).

Vitor H. Pomin – **Marine Regular Sulfated Homopolysaccharides.** Biopolymers **2009**, Volume 91, Issue 8:601-609.

FUCANOMICS & GALACTANOMICS: STRUCTURE *vs* FUNCTION

Structure-anticoagulant activity relationship: CONFORMATIONAL BINDING PREFERENCE

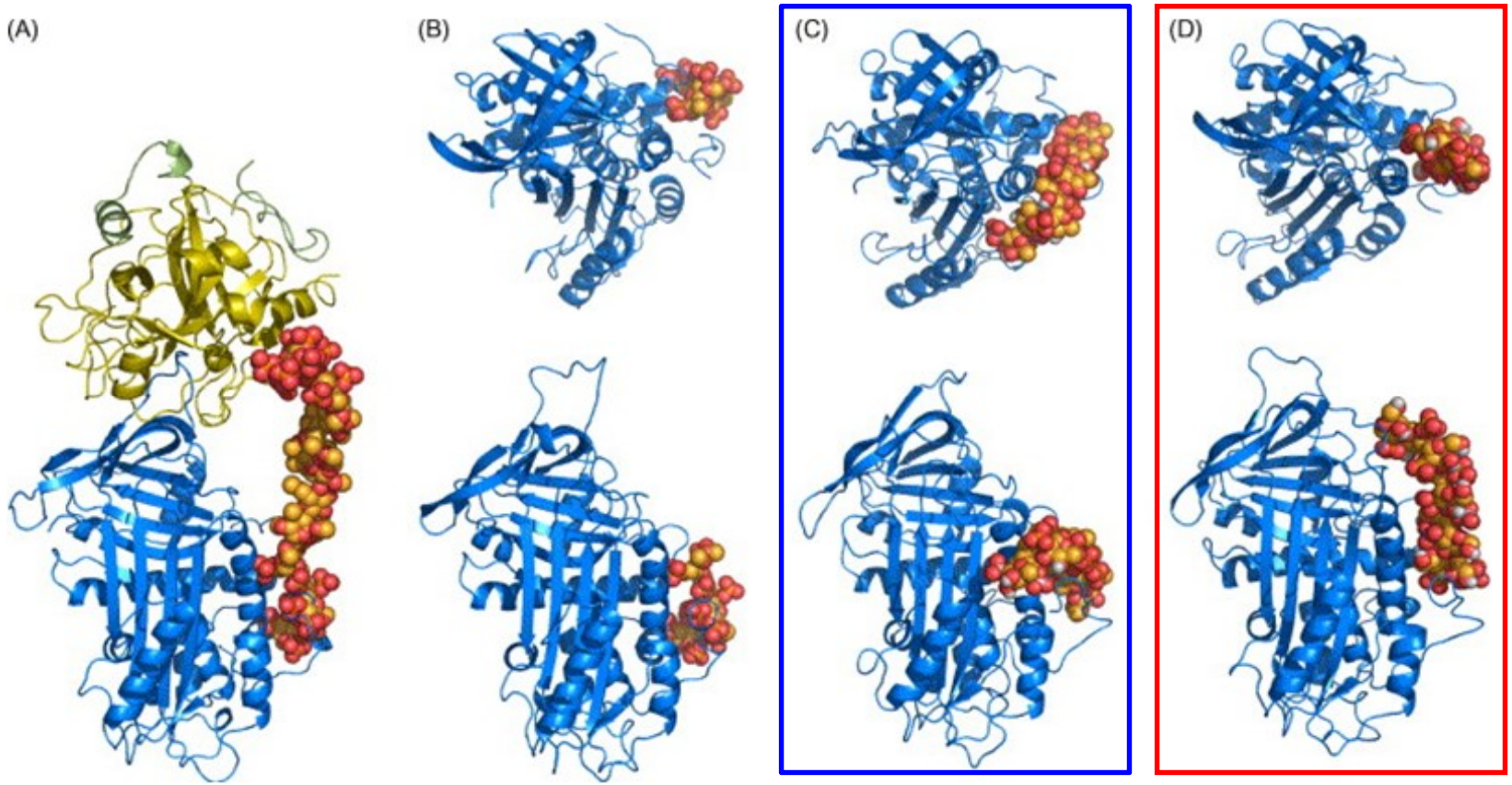

Structures of the complexes between different SP (red, yellow) and AT (blue). (A) ternary complex between AT, thrombin (gold) and a heparin hexadecasaccharide (PDB ID 1TB6); (B) AT bonded to the synthetic pentasaccharide (PDB ID 1E03); (C) final structure from a 5 ns MD of AT complexed to a SF decasaccharide with pyranose rings; (D) final structure from a 5 ns MD of AT complexed to a SG decasaccharide with pyranose rings. For (B)–(D), two orientations of the complexes are presented.

Vitor H. Pomin – **Marine Regular Sulfated Homopolysaccharides.** Biopolymers **2009**, Volume 91, Issue 8:601-609.

Biopolymers

Bloch equations of motion (T_1 and T_2)

- Relaxation processes occur during precession, so the Bloch equations are typically written to account for relaxation

$$\frac{d\vec{M}}{dt} = \gamma \vec{M}(t) \times \vec{B} - (M_z - M_0)(1/T_1) - M_{x,y}(1/T_2)$$

- The component equations are then written as shown, and simplified assuming $B_x = B_y = 0$, and $B_z = B_0$

$$\frac{dM_x}{dt} = \gamma\left(M_y(t)B_z - M_z(t)B_y\right) - \frac{M_x(t)}{T_2} = \gamma M_y(t)B_0 - \frac{M_x(t)}{T_2}$$

$$\frac{dM_y}{dt} = \gamma\left(M_z(t)B_x - M_x(t)B_z\right) - \frac{M_y(t)}{T_2} = -\gamma M_x(t)B_0 - \frac{M_y(t)}{T_2}$$

$$\frac{dM_z}{dt} = \gamma\left(M_x(t)B_y - M_y(t)B_x\right) - \frac{M_z(t) - M_0}{T_1} = -\frac{M_z(t) - M_0}{T_1}$$

Bloch equations of motion (T_2)

- The solutions for M_x and M_y describe the exponential decay, as a function of T_2 (i.e. T_2^*), of the magnitude of the projection of the bulk magnetization vector in the transverse (x-y) plane

$$M_x(t) = \left[M_{x,0}\cos(\omega_0 t) - M_{y,0}\sin(\omega_0 t) \right] e^{(-t/T_2)}$$
$$M_y(t) = \left[M_{y,0}\cos(\omega_0 t) + M_{x,0}\sin(\omega_0 t) \right] e^{(-t/T_2)}$$

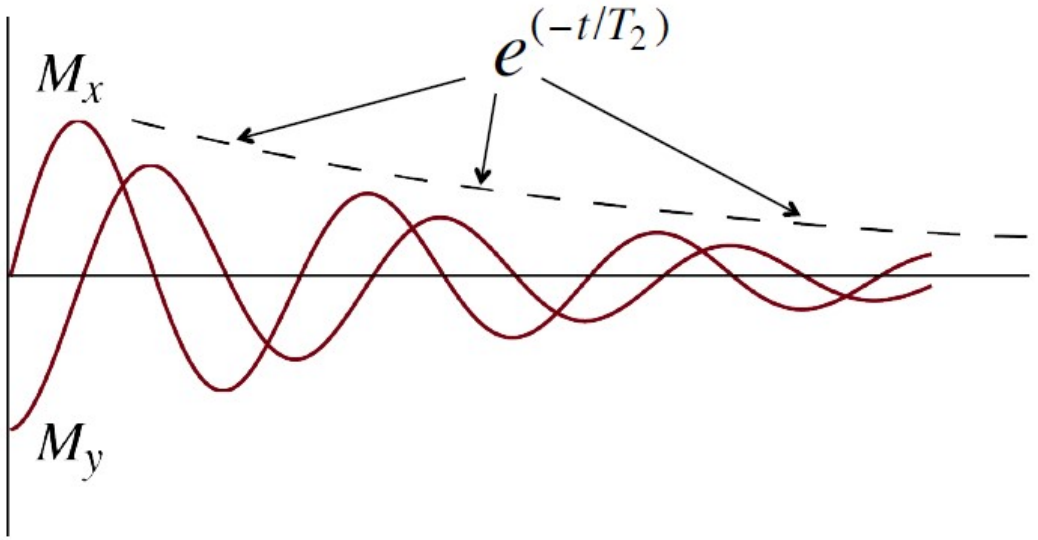

Bloch equations of motion (T_1)

- The solution for M_z describes the exponential growth, as a function of T_1, of M_z along the +z axis, returning to its equilibrium value of M_0 following an RF pulse

$$M_z(t) = M_0 + \left[M_{z,0} - M_0\right]e^{(-t/T_1)} = M_{z,0}e^{(-t/T_1)} + M_0(1 - e^{(-t/T_1)})$$

  - examples: following a 90° pulse ($M_{z,0}$= 0)

$$M_z(t) = M_0(1 - e^{(-t/T_1)})$$

  - examples: following a 180° pulse ($M_{z,0}$= -M_0)

$$M_z(t) = M_0(1 - 2e^{(-t/T_1)})$$

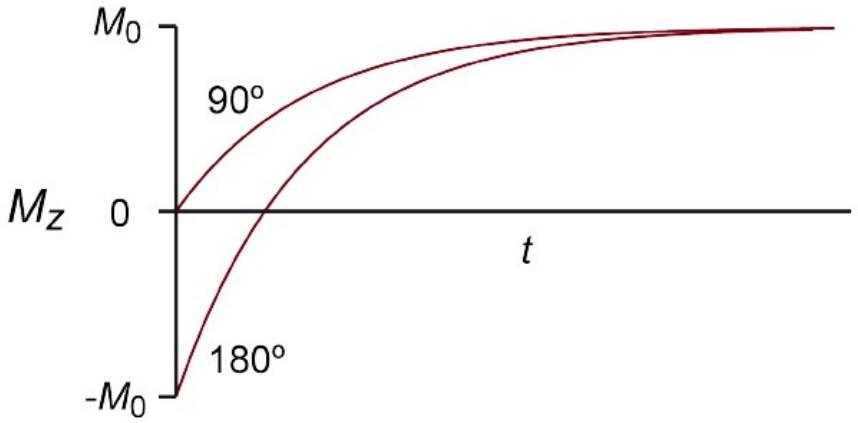

Measuring T_2 by line width or CPMG

- *Spin-spin or Transverse relaxation*
  - While peak width is related to T_2, not an accurate way to measure T_2

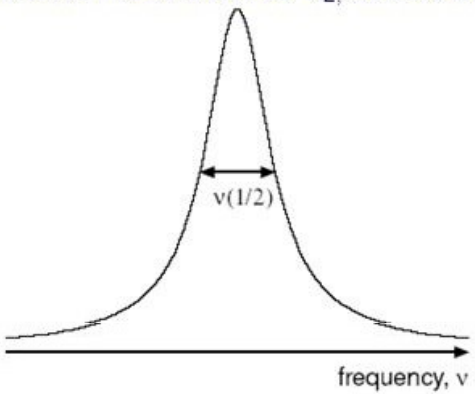

$$\nu_{1/2} = \frac{1}{\pi T_2}$$

  - Use the Carr-Purcell-Meiboom-Gill (CPMG) experiment to measure "spin-echo"
    - Refocuses spin diffusions due to magnetic field inhomogeneiety

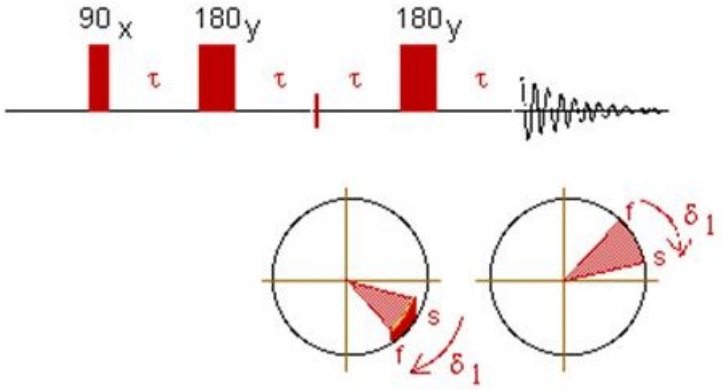

CPMG

- The **Carr-Purcell-Meiboom-Gill sequence (CPMG) experiment** allows to measure transverse or spin-spin T_2 relaxation times of any nucleus.
- The experimental half-height line width (d) of a given resonance is directly related to T_2^* by the equation

$d=1/(pi.T_2^*)$.

- In the measurement of the T_2 relaxation times, the magnetic field inhomogeneities (T_2^{inh}) must be considered:

$1/T_2^* = (1/T_2) + (1/T_2^{inh})$.

CPMG pulse sequence

- The basic pulse sequence of the CPMG experiment is based on the spin-echo pulse sequence and consists of the following steps: (1) a 90º pulse creates transverse magnetization; (2) an *spin-echo period* (delay-180º-delay block) repeated n times, which determines the decay of the M_{xy} magnetization; and (3) signal acquisition performed as usual.

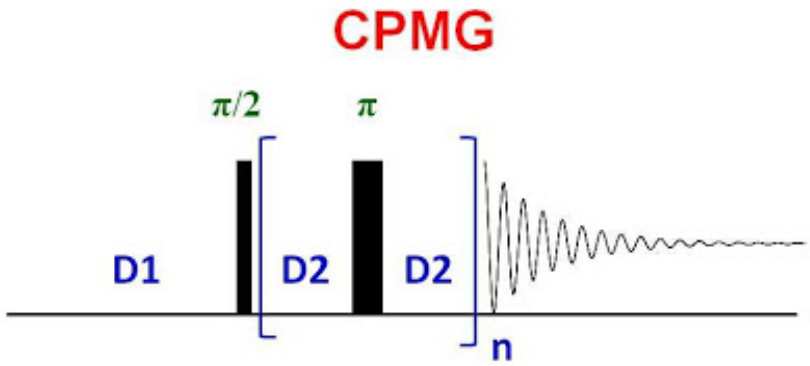

T_2 measurements with a Simple Hahn Echo or Spin Echo

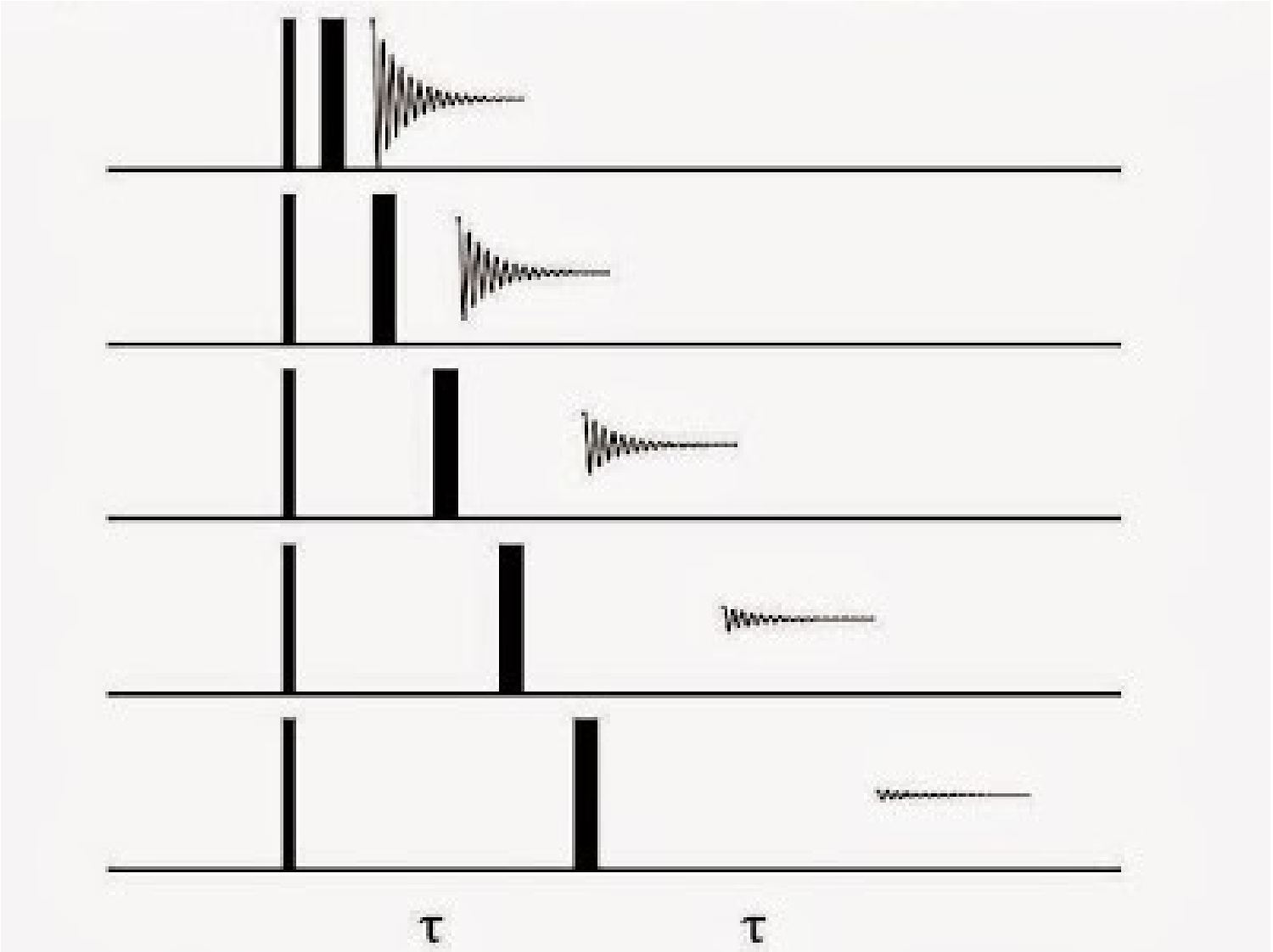

Hahn Echoes as a Function of Inhomogeneous Line Width

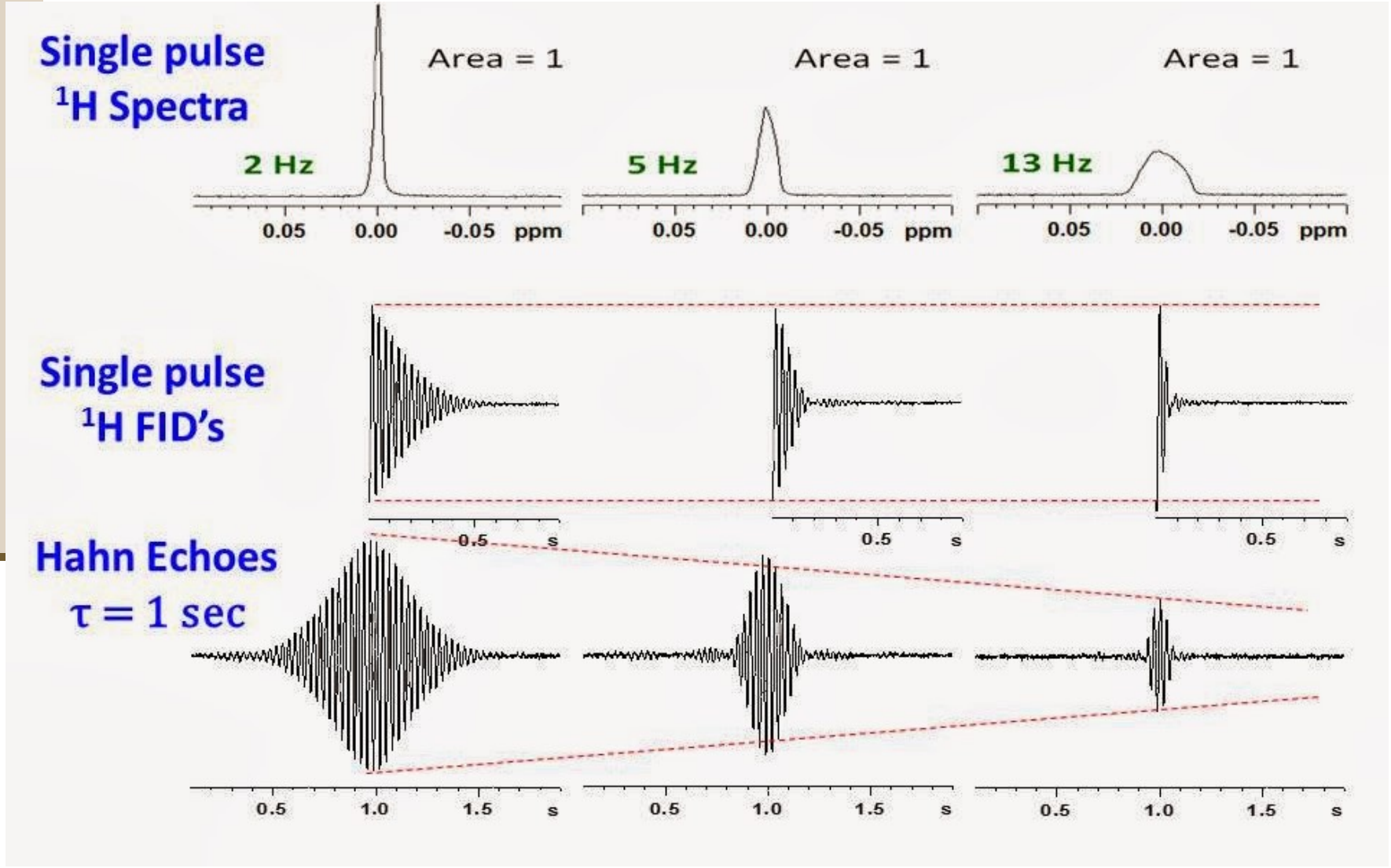

T_2 Measurement with a CPMG Spin Echo Train

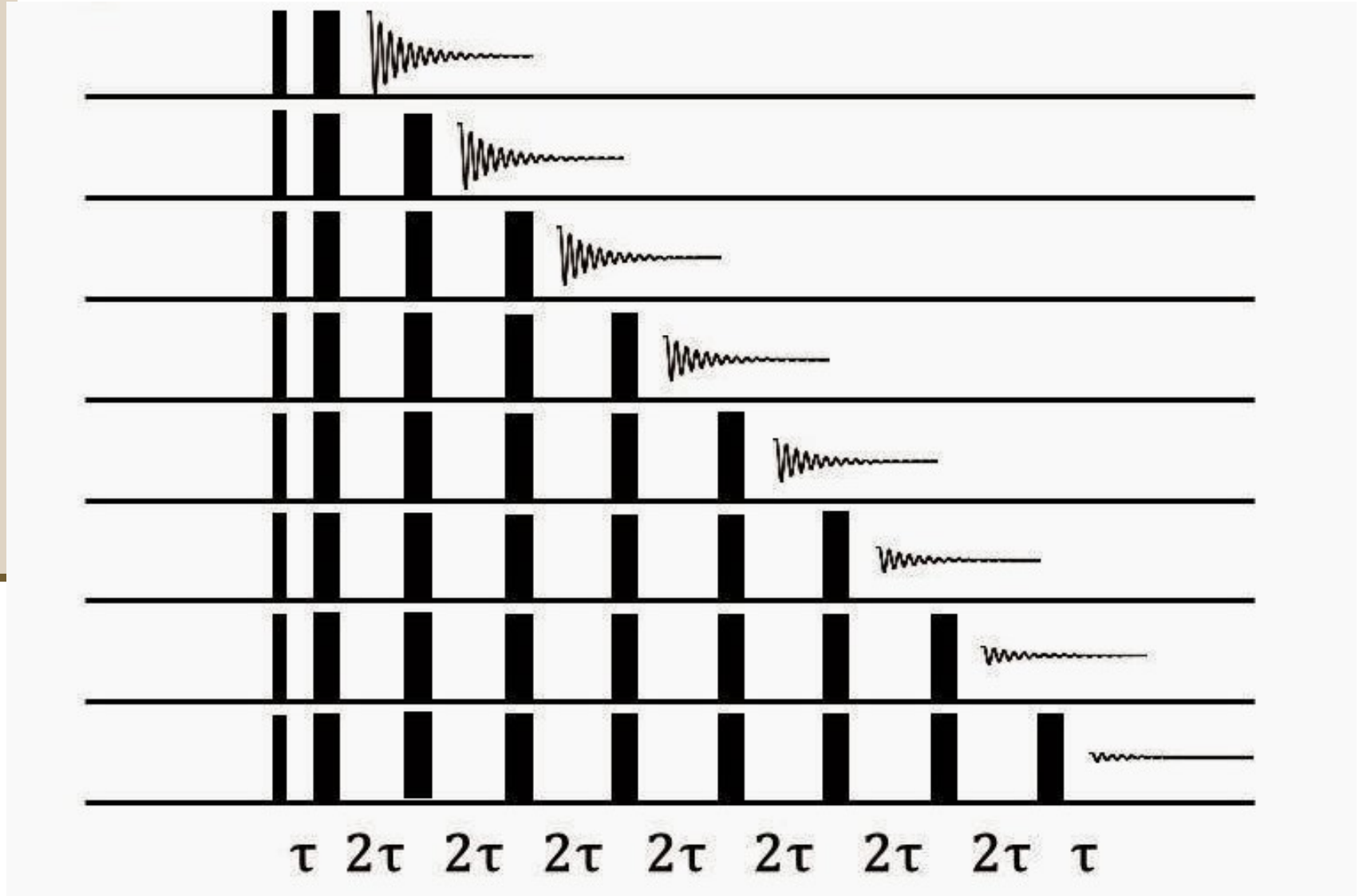

The Spin Echo through CPMG

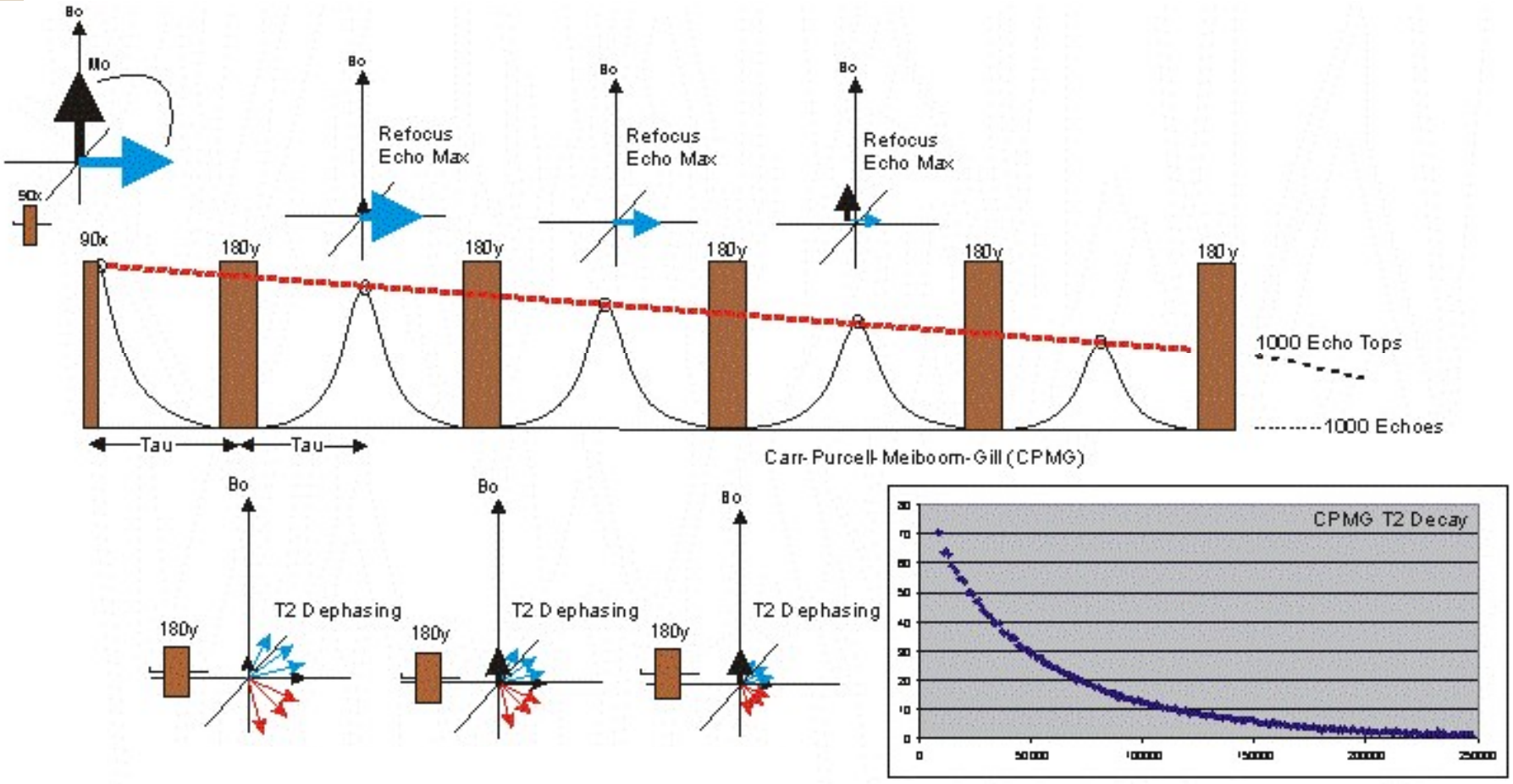

CPMG: T_2 vs T_2*

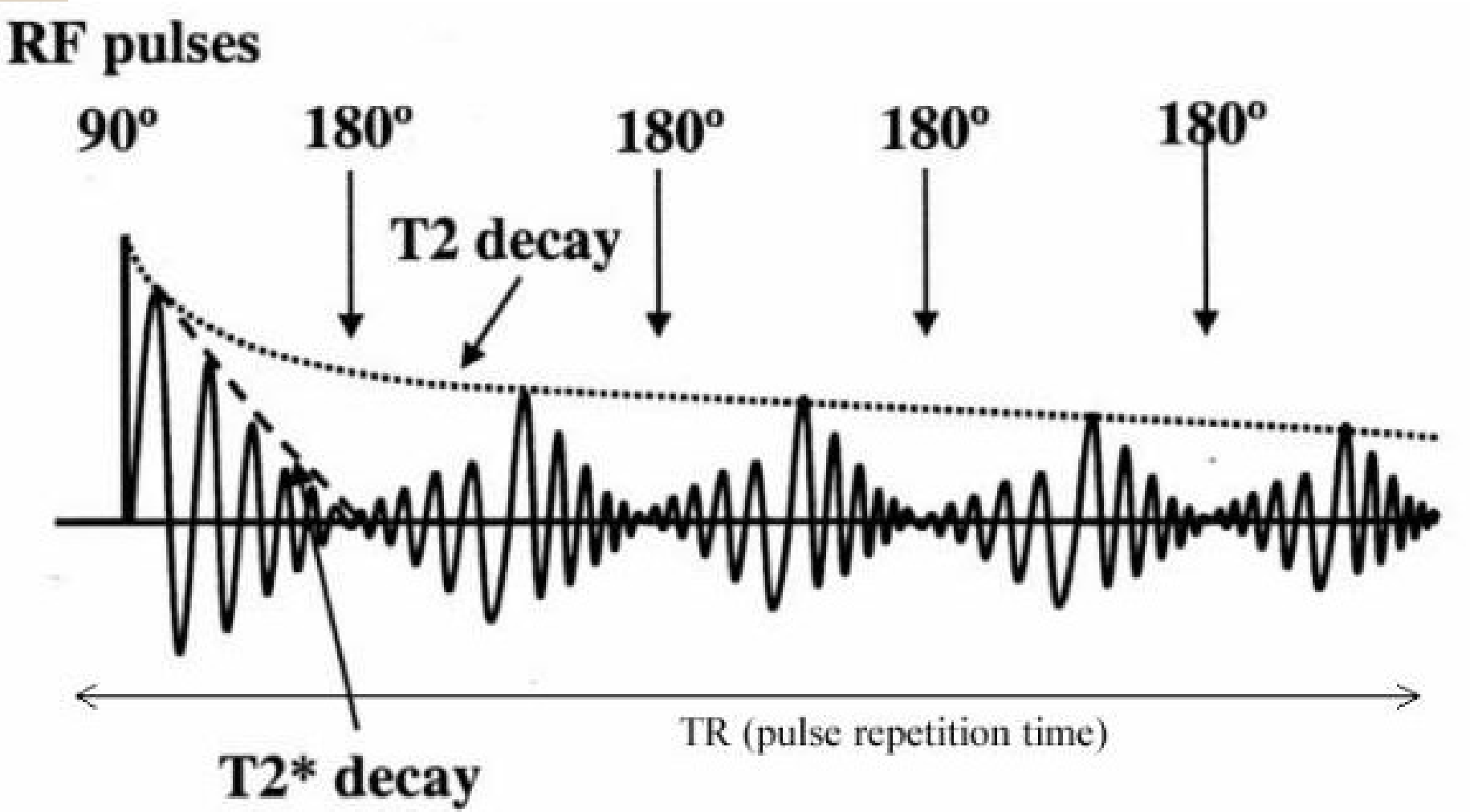
RF pulses
90°
180°
180°
180°
180°
T2 decay
T2* decay
TR (pulse repetition time)

T_2 vs T_2*

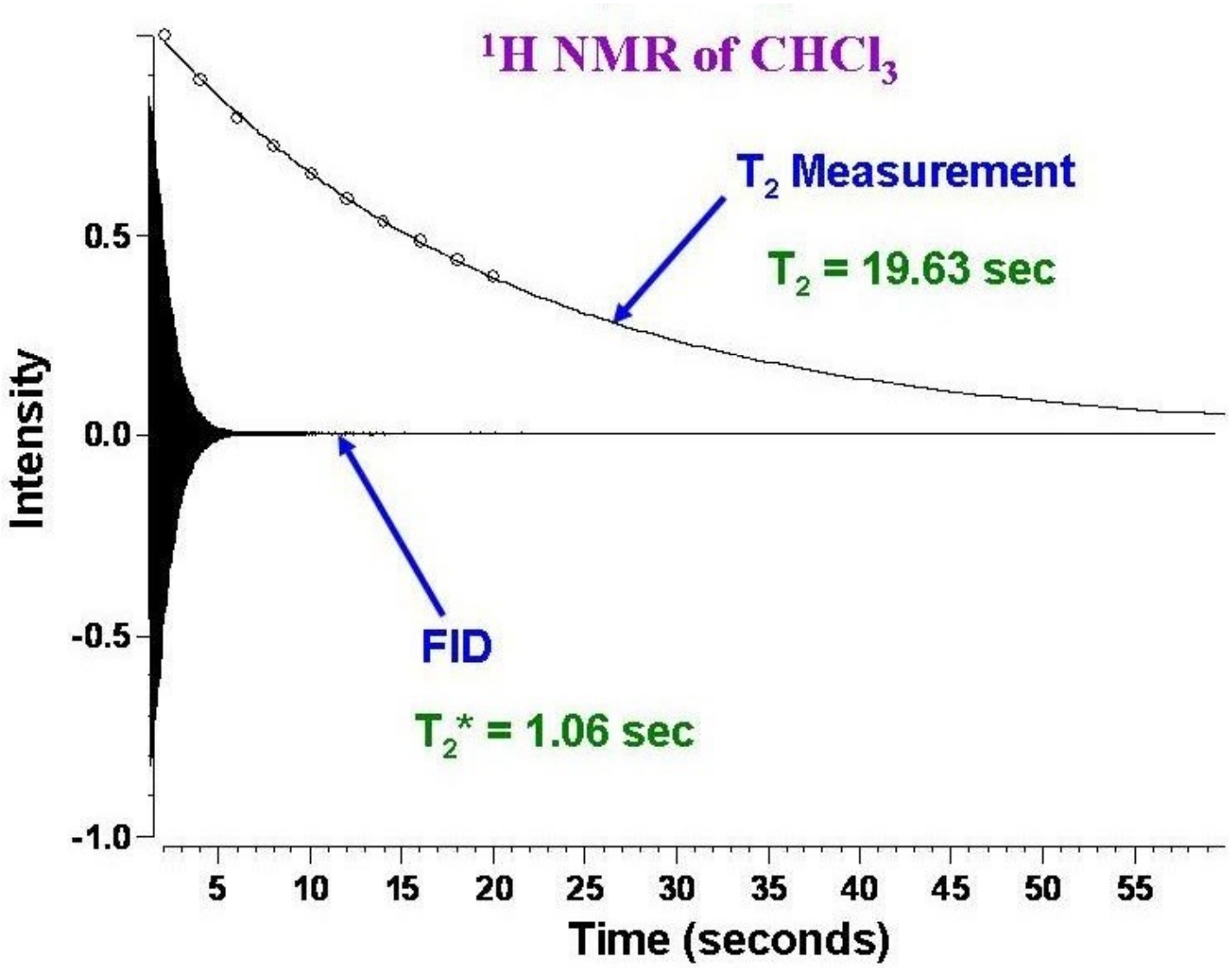
^{1}H NMR of $CHCl_3$
T_2 Measurement
T_2 = 19.63 sec
FID
T_2* = 1.06 sec
Intensity
0.5
0.0
-0.5
-1.0
5
10
15
20
25
30
35
40
45
50
55
Time (seconds)

CPMG: examples

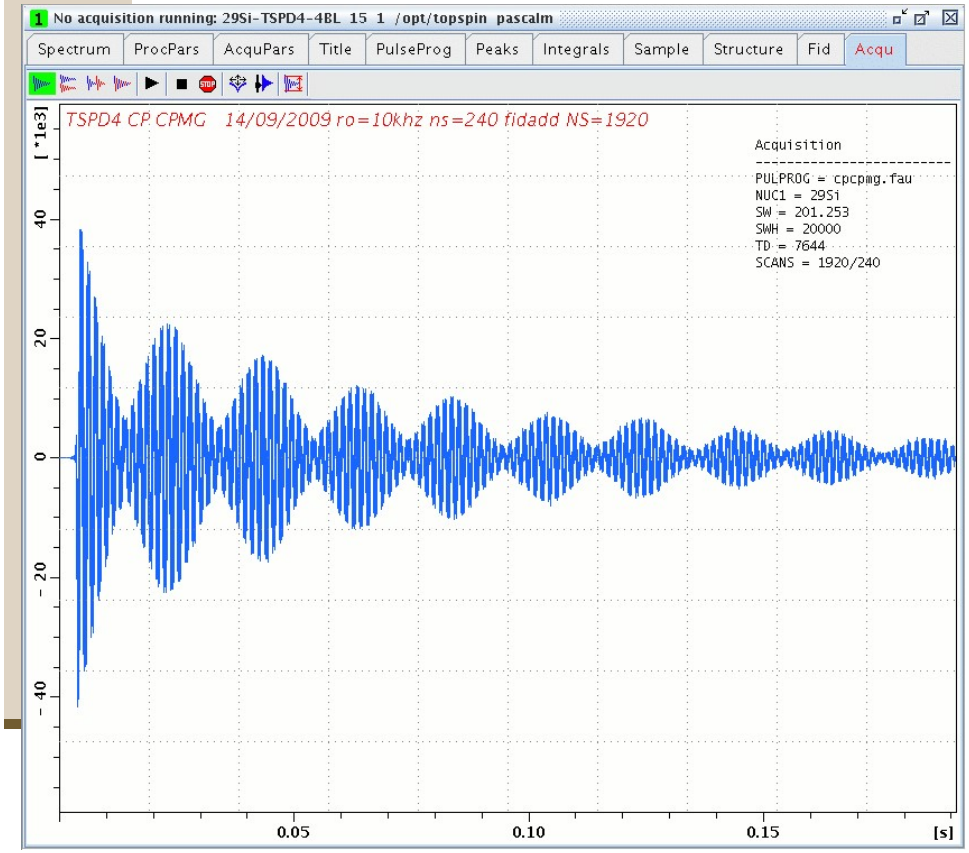

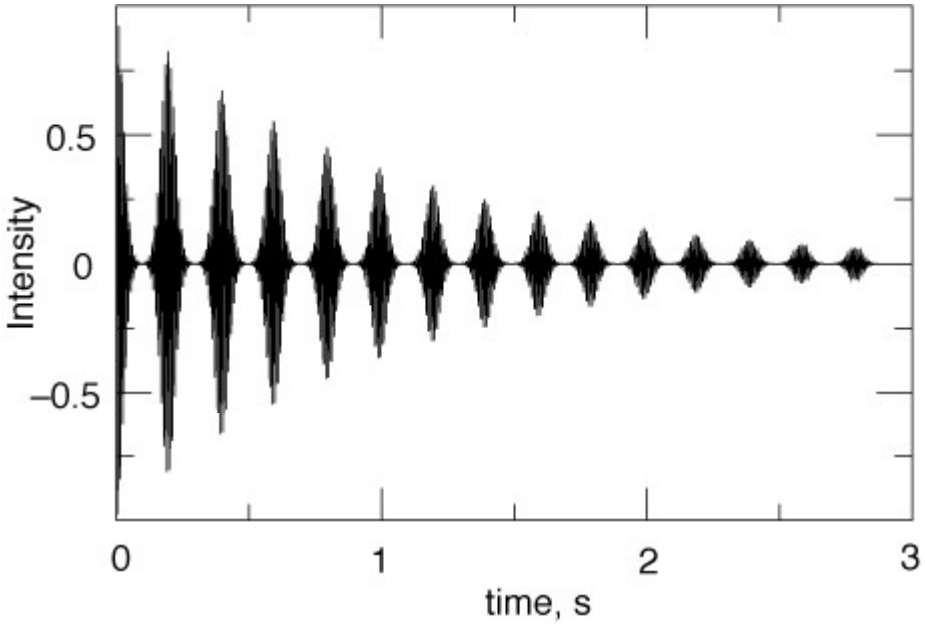

Measuring T_1 by Inversion Recovery

- Measurement of T_1 is important, as the relaxation rate of different nuclei in a molecule can tell us about their local mobility. We cannot measure it directly on the signal or the FID because T_1 affects magnetization we don't detect. We use the following pulse sequence:

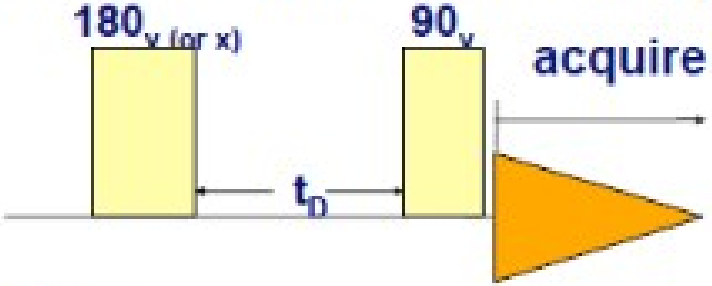

- analyze after the π pulse:

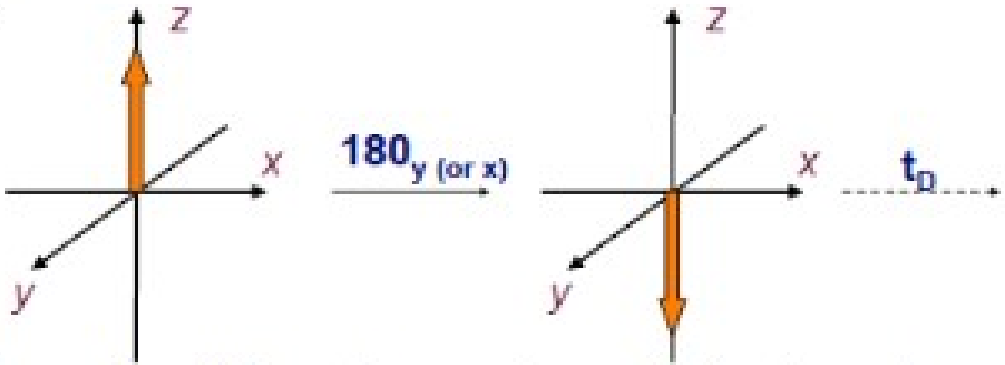

- we are letting the signal decay by different amounts exclusively under the effect of longitudinal relaxation (T_1), we'll see how different t_D's affect the intensity of the FID and the signal after FT.

Measuring T_1 by Inversion Recovery

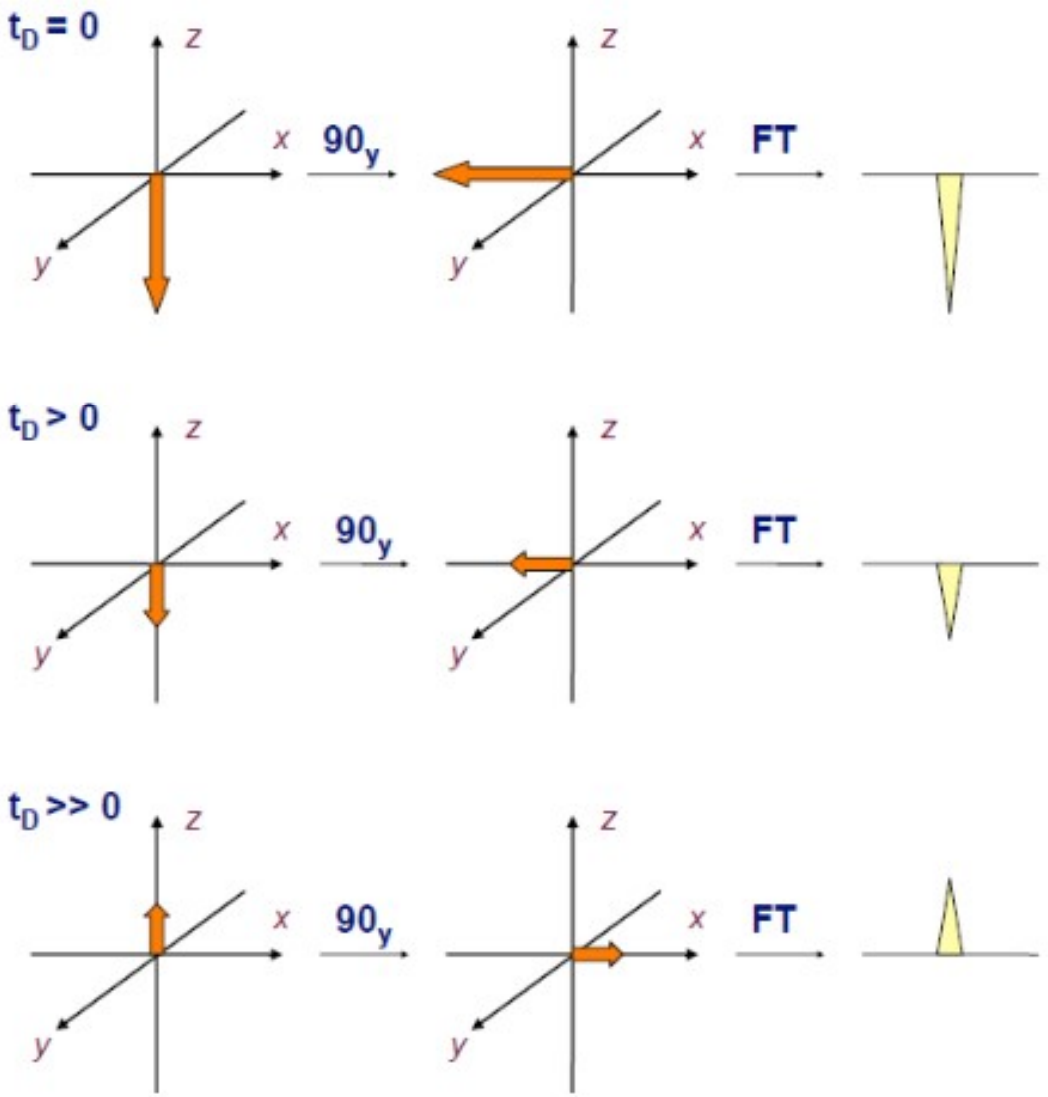

Measuring T_1 by Inversion Recovery

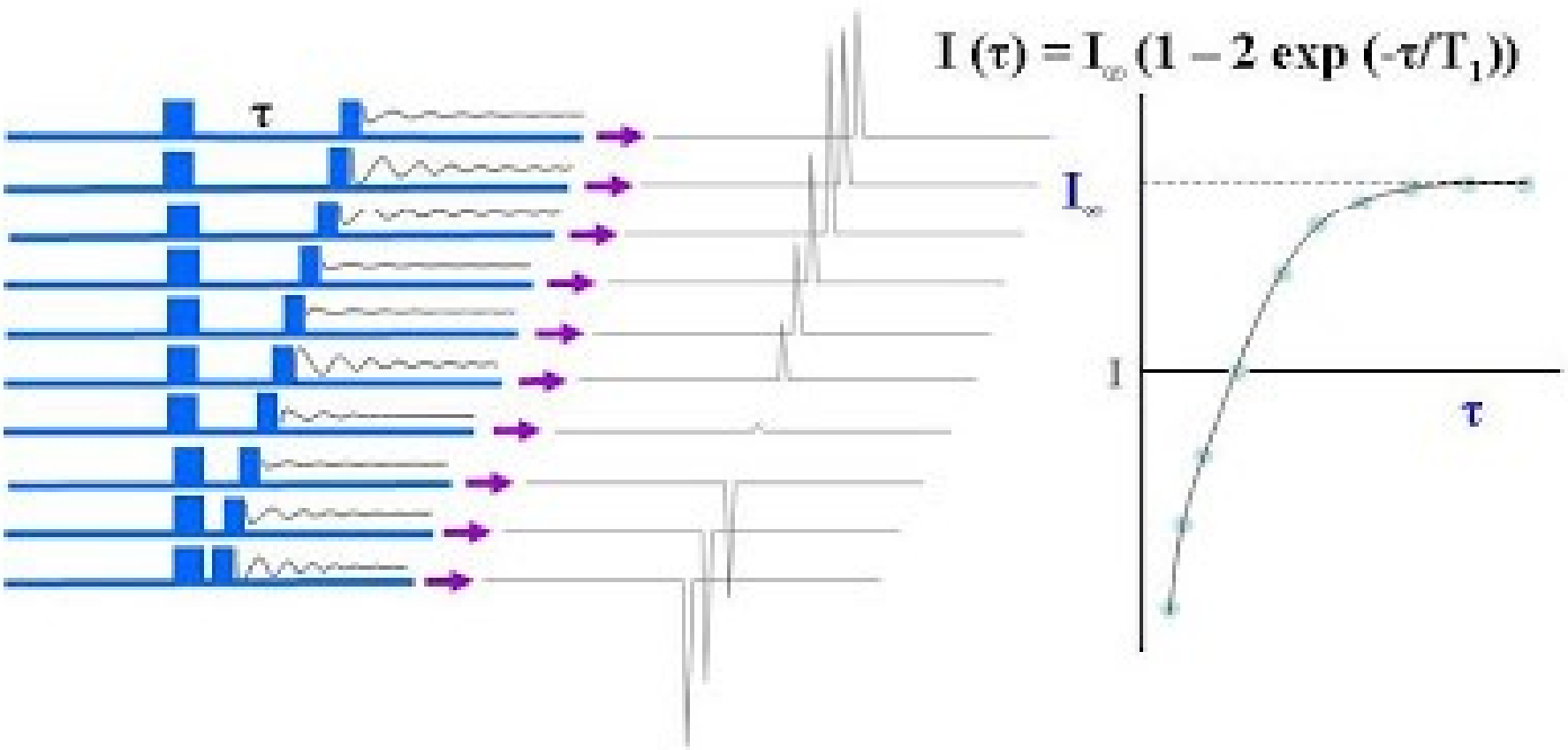

Spin Echo (T_2) vs Inversion Recovery (T_1)

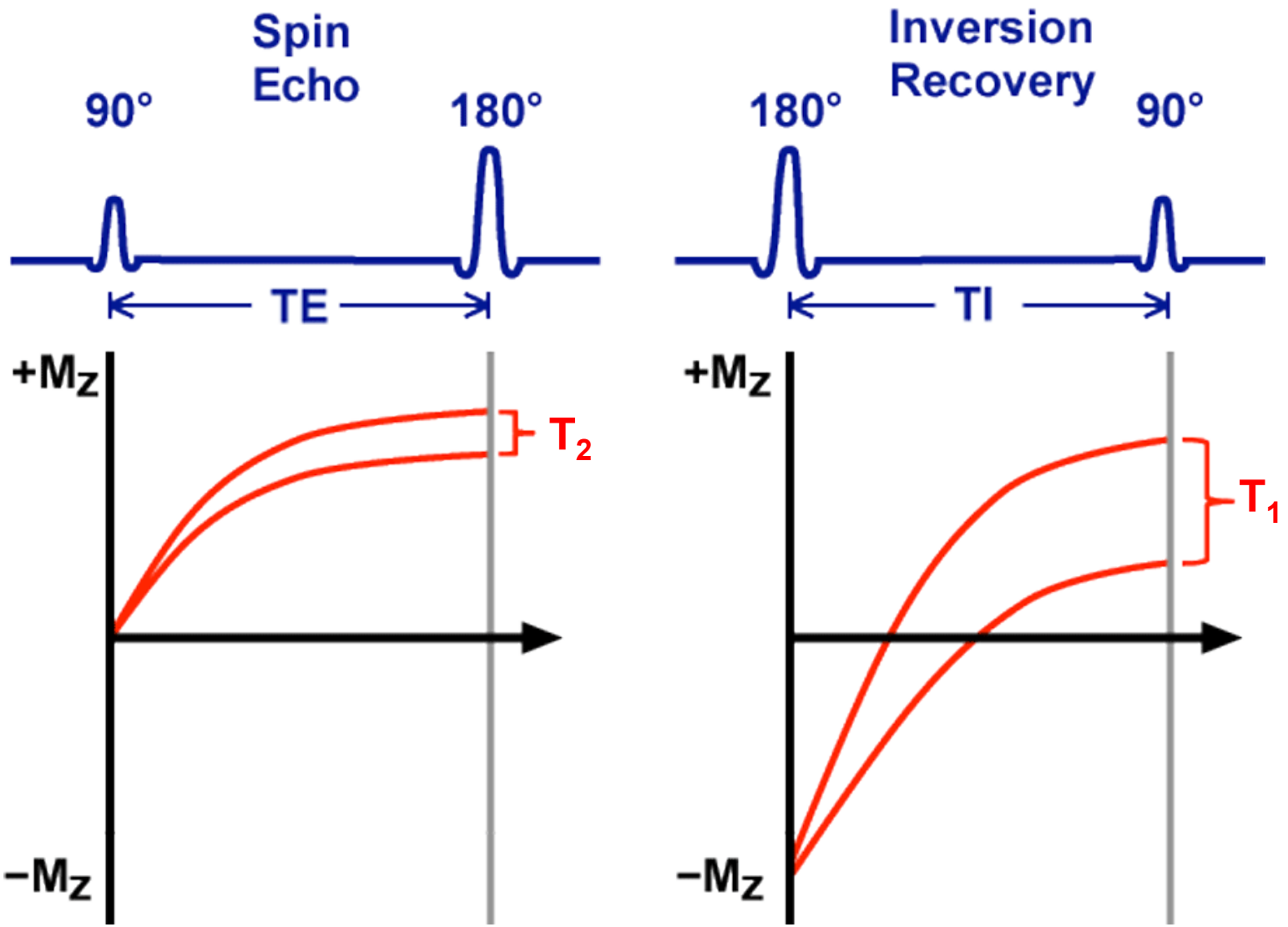

T_1 from Inversion Recovery in MRI